Chinese Chemical Letters 34 (2023) 107626

Contents lists available at ScienceDirect

Chinese Chemical Letters

journal homepage: www.elsevier.com/locate/cclet

Multi-organelle-targeting pH-dependent NIR fluorescent probe for lysosomal viscosity

Huili Wang[a,1], Yishuo Sun[b,1], Xuemei Lin[a], Wei Feng[b], Zhanxian Li[a,*], Mingming Yu[a,*]

[a] Green Catalysis Center and College of Chemistry, Zhengzhou University, Zhengzhou 450001, China
[b] Department of Chemistry, State Key Laboratory of Molecular Engineering of Polymers, Institutes of Biomedical Sciences & Collaborative Innovation Center of Chemistry for Energy Materials, Fudan University, Shanghai 200433, China

ARTICLE INFO

Article history:
Received 30 March 2022
Revised 17 June 2022
Accepted 20 June 2022
Available online 23 June 2022

Keywords:
NIR
Lysosomal viscosity
PH-dependent
Multi-organelle localization

ABSTRACT

The normal operation of lysosome, mitochondria, Golgi apparatus and endoplasmic reticulum plays a significant role in maintaining cell homeostasis. Reflecting the state and function of lysosomes, viscosity is a pivotal parameter to assess the stability of microenvironment. Herein, based on TICT mechanism, a new NIR pH-dependent fluorescent probe DCIC with push-pull electronic moiety was synthesized to identify the lysosomes viscosity. In viscous media, DCIC was highly sensitive to viscosity, fluorescence intensity increased by 180 times as viscosity increased from 1.0 cp to 438.4 cp. In addition, DCIC have high localization ability for lysosome, mitochondria, Golgi apparatus, and endoplasmic reticulum and can monitor lysosomal viscosity fluctuations with laser confocal microscopy.

Lysosomes are digestive organs of cells, capable of removing damaged organelles and digesting various endogenous and exogenous biological macromolecules, which play a vital role in maintaining cell homeostasis [1,2]. Mitochondria, as the "energy factory" of cells, not only participate in the production of adenosine triphosphate (ATP), but also regulate cell growth, cycle and apoptosis, which are closely related to cell senescence and occurrence of tumors [3–5]. The endoplasmic reticulum (ER), possessing the largest membrane area compared with other organelles, is an indispensable part of eukaryotic cells for being involved in plenty of biological processes, including exogenous metabolism and protein synthesis [6–9]. The Golgi apparatus is a transporter organelle which can manage and transport abundant proteins synthesized by the ER, delivering them to other organelles or secreting them outside the cells [10,11]. The normal function of these organelles is fundamental to the maintenance of cellular homeostasis and health of organism. The stability of intracellular microenvironment provides basis for the normal operation of organelles. As a crucial factor affecting the stability of microenvironment, viscosity plays an important role in biomolecular interactions, enzyme catalysis, signaling and other biological diffusion processes [12–14]. Abnormal viscosity levels are associated with a variety of diseases, including diabetes, cardiovascular disease, and even cancer [10,15].

Traditional methods of viscosity measurement using mechanicals, such as rotary viscometer, can only be used to measure viscosity of macroscopic materials. In recent years, fluorescent probe technology has been popular with researchers because of its non-invasiveness, *in situ*-imaging, real-time detection, high analytical sensitivity and other advantages. Researchers have developed various viscosity fluorescent probes based on molecular rotors, and these probes exhibit enhanced fluorescence or prolonged fluorescence lifetime as the system viscosity increases [16–18]. However, the practical application of many probes which emit green or blue fluorescence is limited due to short emission wavelength and poor tissue penetration [19,20]. Moreover, many viscosity fluorescent probes targeting lysosomes are highly dependent on acidic pH environment, and may lose their ability to trace lysosome when pH increases owing to the resumption of photoinduced electron transfer (PET) processes [21–23]. Due to its long emission wavelength, the near infrared fluorescent (NIR) probe has the advantages of deep tissue penetration, little background fluorescence interference and weak fluorescence background [10,24,25]. Therefore, development of near-infrared viscosity fluorescence probes with multi-organelle localization ability is of great significance for biological imaging and disease diagnosis.

In this contribution, DCIC (Scheme 1) was prepared by coupling cyanogen modified hemicyanine group and pyrrolidine modified coumarin group. The pyrrolidine modified coumarin unit served as an electron donor, and the cyanogen modified hemicyanine acted as an electron-withdrawing group, which make DCIC capable of

* Corresponding authors.
E-mail addresses: lizx@zzu.edu.cn (Z. Li), yumm@zzu.edu.cn (M. Yu).
[1] These authors contributed equally to this work.

https://doi.org/10.1016/j.cclet.2022.06.049
1001-8417/

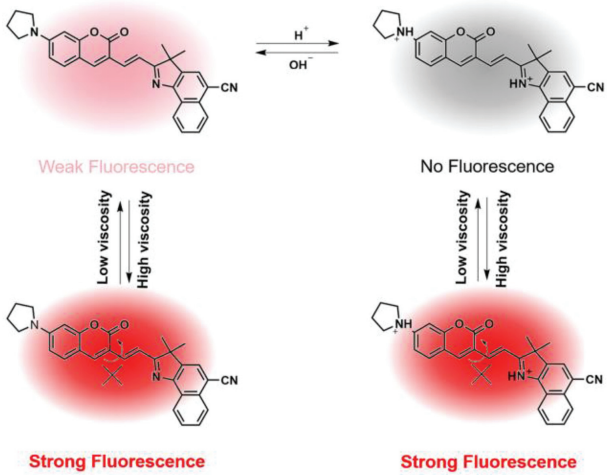

Scheme 1. Molecular structure of probe DCIC and the proposed viscosity sensing mechanism.

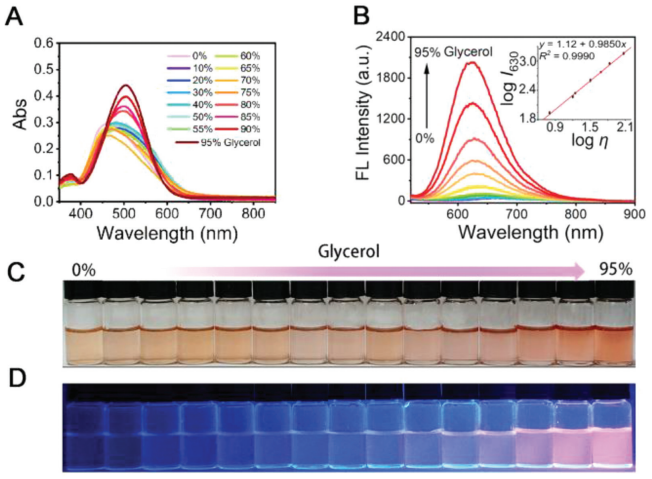

Fig. 1. (A) UV–vis absorption spectra of probe DCIC (10 μmol/L) in PBS-glycerol mixed solvents. (B) Fluorescence spectra of probe DCIC (10 μmol/L) in PBS-glycerol mixed solvents, insert: the picture of linear relationship between the log of maximum emission intensity of DCIC at 630 nm (log I_{630}) and log η (viscosity), λ_{ex} = 500 nm, slits: 5/5 nm. (C) The color change of DCIC in PBS-glycerol mixed solvents in the natural light and (D) the light of 365 nm portable UV lamp.

Table 1
Photophysical properties of DCIC.

Solvent	$\lambda_{abs,max}$ (nm)	$\lambda_{em,max}$ (nm)	Stokes shift	ε (L moL^{-1} cm^{-1})	QY (%)
DMSO	496	625	129	47,100	3.90
DMF	493	615	122	60,200	2.02
MeOH	490	617	127	34,500	1.08
EtOH	491	614	123	31,300	0.90
Acetone	486	605	119	51,900	1.29
CH_3CN	489	614	125	50,700	1.10
THF	491	600	109	67,600	1.27
EA	478	600	122	64,900	0.92
DCM	486	608	122	67,400	0.88
$CHCl_3$	484	599	115	65,700	0.85
Glycerol	505	620	115	47,000	19.69

viscosity sensitivity based on twisted intramolecular charge transfer. The steps for synthesis of DCIC are shown in Scheme S1 (Supporting information). Compounds C1, C2, D1 and D2 are prepared according to our previous work [26]. Unlike many pH-dependent lysosomal viscosity probes, fluorescence quenching of DCIC did not occur with environment changing from acidic to neutral or alkaline, providing the basis for multi-organelle localization. Besides, DCIC also has the advantages of long emission wavelength, large Stokes shift, high photostability and low cytotoxicity. These features enable DCIC to locate lysosomes, mitochondria, Golgi, and ER in cells and monitor lysosomal viscosity changes.

The photophysical property of DCIC was first investigated in various organic solvents. As depicted in Fig. S1A (Supporting information), the maximum absorption wavelength of probe DCIC dissolved in DMSO, DMF, MeOH, EtOH, Acetone, CH_3CN, THF, EA, CH_2Cl_2, $CHCl_3$ and glycerol was around 500 nm. Therefore, the corresponding fluorescence emission spectrum was measured using 500 nm as the excitation wavelength. Fluorescence intensity of DCIC in glycerol was obviously strong, comparing with the weak fluorescence in DMSO, DMF, EtOH, CH_2Cl_2 and other low-viscosity organic solvents (Fig. S1B in Supporting information). Besides, as depicted in Table 1, fluorescence quantum yield of DCIC in glycerol (φ = 19.69%) is much higher than those observed in other organic solvents. These results show that probe DCIC can respond to viscosity without polarity interference.

The sensitive response of DCIC toward viscosity was investigated in PBS-glycerol solvents with volume ratio of glycerol increased from 0 to 95 (1.0–438.4 cp). With the increase of solvent viscosity, the absorption intensity of DCIC showed a general enhancement, and a slight red-shift of the maximum absorption wavelength appeared, which can be ascribed to a lower energy transition caused by enlarged conjugate planar (Fig. 1A). Meanwhile, fluorescence intensity of DCIC at 630 nm increased gradually and showed 83 times enhancement in 95% glycerol compared with that in pure PBS (Fig. 1B). The recovery of fluorescence could be attributed to the high viscosity of glycerol limiting the intramolecular rotation speed of hemicyanine and coumarin moieties along vinyl group. Correspondingly, it can be observed under naked eyes that the color of DCIC solution changed from light-orange to deep-orange and under the irradiation of 365 nm portable UV lamp, fluorescence color became stronger with the increase of solution viscosity (Figs. 1C and D). In addition, by fitting the Forster-Hoffmann equation (Fig. 1B, inset), there was an excellent linear relationship between fluorescence intensity (log I_{630}) and viscosity (log η) of DCIC (R^2 = 0.99, x = 1.12). All these findings illustrate that probe DCIC was able to indicate solution viscosity quantitatively.

In order to investigate the effect of pH on the fluorescence response performance of DCIC, the UV–vis spectra and fluorescence spectra of DCIC in PBS buffer solutions with increasing pH values were tested. As shown in Fig. S2 (Supporting information), fluorescence intensity enhanced for 5 times when pH of the solution changed from 8 to 2. Because DCIC possesses both pyrrolidine nitrogen and hemicyanine nitrogen, it was difficult to determine which nitrogen atom affected fluorescence emission. In order to find out the structural and conformational changes during acidity enhancement, Trifluoroacetic acid (TFA) was titrated into solution of DCIC to confirm which nitrogen atom was protonated. The results in Fig. 2 showed that there were obviously gradual downfield shifts of proton peaks in coumarin scaffold in addition to hemicyanine scaffold after adding TFA, except for the proton peak at the n position, indicating that when acidity increased, both pyrrolidine nitrogen atom and indole nitrogen atom were protonated [27], resulting in fluorescence quenching of DCIC. The fluorescence response in solutions with different viscosity at different pH was tested to further explore the effect of viscosity and pH on DCIC. The result in Figs. 3A and B showed that when the pH of DCIC solution was the same, the fluorescence of DCIC enhanced as viscosity increased; when the viscosity was constant, except for pure PBS solution, the fluorescence spectrum of the probe DCIC kept almost identical in the range of pH 3–9. These results indicated that when

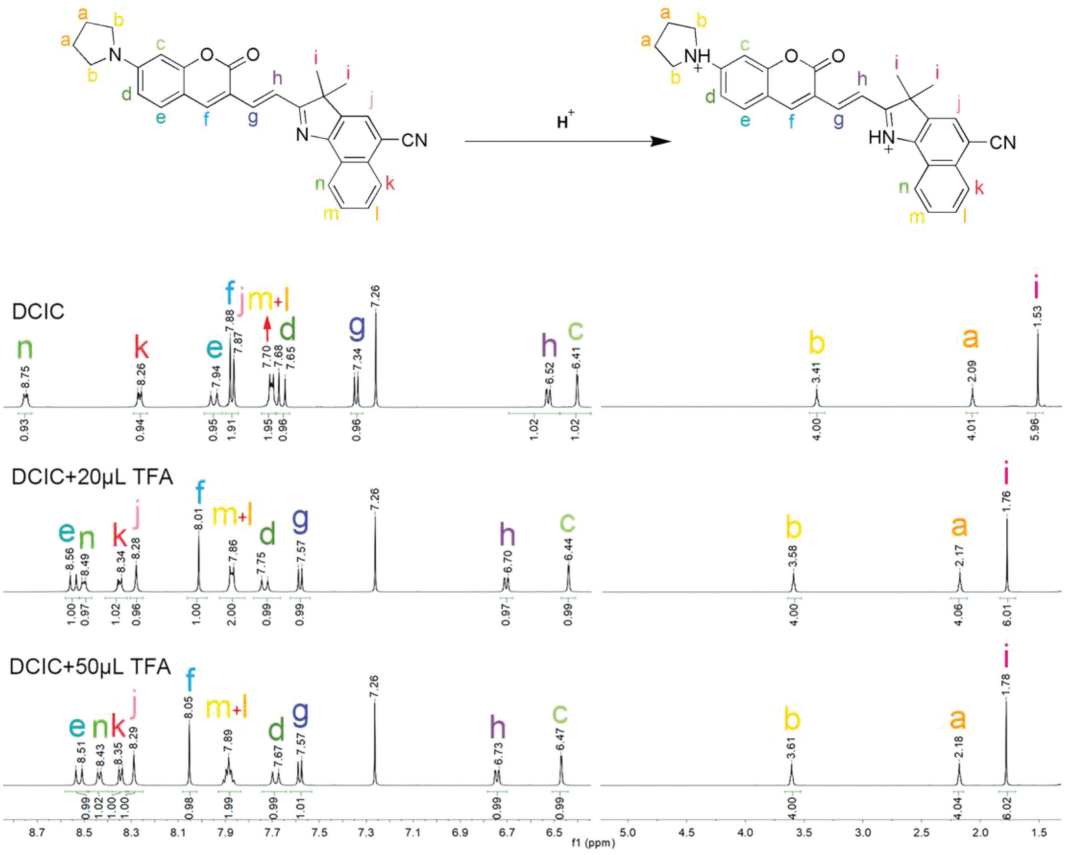

Fig. 2. ^{1}H NMR (600 MHz, $CDCl_3$) spectroscopic titration of DCIC with trifluoroacetic acid (TFA).

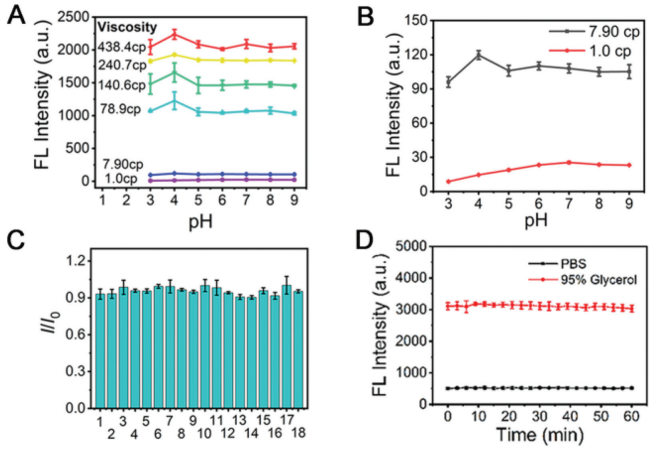

Fig. 3. (A) Fluorescence intensity of DCIC (10 μmol/L) at 630 nm in PBS/glycerol mixed solvents at different pH (3–9) and viscosity (1.0–438.4 cp). (B) Fluorescence intensity of DCIC (10 μmol/L) at 630 nm in PBS buffer solution (1.0 cp) and PBS/glycerol mixed solvents (7.9 cp) at different pH (3–9). (C) Fluorescence intensity ratio of DCIC (10 μmol/L) upon addition of different biologically relevants (3 μL, 0.1 mol/L), 1. Ca^{2+}, 2. Cu^{2+}, 3. Fe^{2+}, 4. Fe^{3+}, 5. K^{+}, 6. Mg^{2+}, 7. Mn^{2+}, 8. Na^{+}, 9. Zn^{2+}, 10. F^{-}, 11. Cl^{-}, 12. S^{2-}, 13. ClO^{-}, 14. $CO_3{}^{2-}$, 15. $HSO_3{}^{-}$, 16. Cys, 17. GSH, 18. H_2O_2. (D) The time-dependent fluorescence changes of DCIC (10 μmol/L) at 665 nm in PBS buffer solution (λ_{ex} =500 nm, slits: 10/10 nm) and in 95% glycerol solution (λ_{ex} =500 nm, slits: 5/5 nm), respectively.

viscosity was high, the pH-dependence of DCIC would be weakened and the TICT effect would be enhanced. Moreover, the lysosomes of normal cells are acidic (pH 3.8–5.5) [21,22], so the pH-dependence of DCIC makes it especially suitable for the detection of viscosity in intracellular acidic environment. Unlike the pH dependence of many lysosomal probes [28,29], fluorescence of DCIC was not quenched in neutral and alkaline environments, which also provided the basis for the localization of various organelles.

The cellular microenvironment is a complex system, so probes must have excellent specificity towards viscosity. We added interfering substances to PBS buffer solution of the probe, including Ca^{2+}, Cu^{2+}, Fe^{2+}, Fe^{3+}, K^{+}, Mg^{2+}, Mn^{2+}, Na^{+}, Zn^{2+}, F^{-}, Cl^{-}, S^{2-}, ClO^{-}, $CO_3{}^{2-}$, $HSO_3{}^{-}$, Cys, GSH, H_2O_2. As depicted in Fig. 3C, these species did not cause obvious fluorescence changes of DCIC, indicating that the specificity toward viscosity of DCIC was satisfactory. In addition, the photostability of DCIC was also tested. Fluorescence intensity at 665 nm was barely changed in 60 min no matter in PBS buffer solution or 95% glycerol solution (Fig. 3D), proving that probe DCIC was highly stable.

The cytotoxicity of probe DCIC was examined by the MTT assay before confocal imaging of cells. After 12 h of incubation with varied concentrations of DCIC in HeLa cells, no obvious cytotoxicity was observed (Fig. S3 in Supporting information), indicating that probe DCIC can be applied to bio-imaging. To verify whether DCIC can localize multiple organelles, we performed colocalization experiments of DCIC with commercial mitochondrial probe (Mitotracker Green), lysosomal probe (Lyso-tracker Green), Golgi probe (Golgi-tracker Green), endoplasmic reticulum probe (ER-tracker Green). Following pretreatment with probe DCIC for 1 h, HeLa cells were then stained with these commercial dyes, respectively, and images were obtained with a laser confocal microscope. As we can see from Fig. 4, cells labeled by DCIC gave red fluorescence and cells labeled by commercial dyes exhibited green fluorescence, respectively. The red image of DCIC in mitochondria, lysosomes, Golgi apparatus and ER merged very well with the green images,

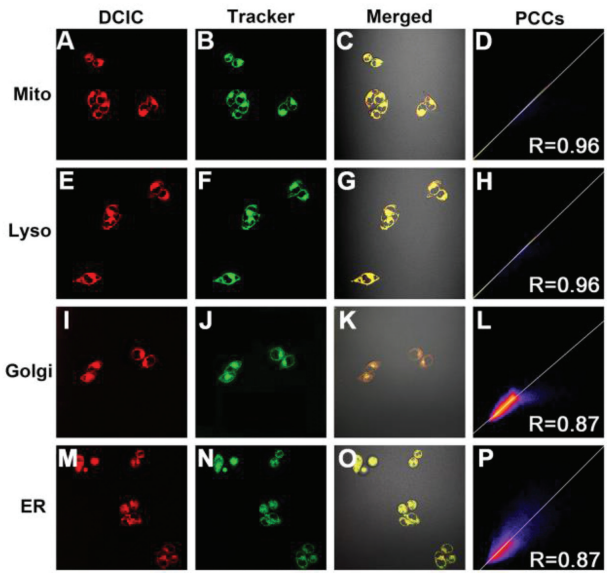

Fig. 4. Cell imaging of DCIC in HeLa cells. (A, E, I, M) Images of DCIC (1 μmol/L) in the red emission channel. (B, F, J, N) Fluorescence from commercial dyes in the green emission channel. (C, G, K, O) Merged images of the red and green channels. (D, H, L, P) The correlation plots of red and green channels.

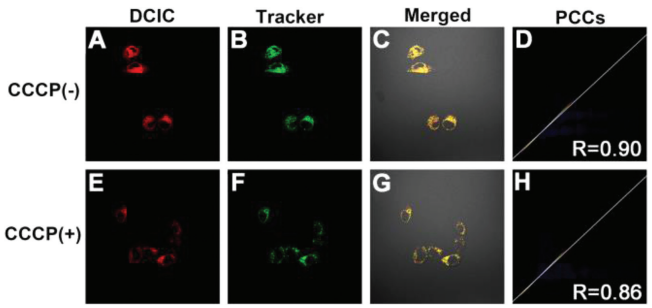

Fig. 5. Fluorescence images of HeLa cells: (A-D) Cells were treated with DCIC (10 μmol/L) and Mito-Tracker Green (1 μmol/L) for 30 min. (E-H) Cells were pretreated with DCIC (10 μmol/L) and Mito-Tracker Green (1 μmol/L) for 30 min, then incubated with CCCP (20 μmol/L) for another 30 min.

resulting obvious yellow images. Additionally, the Pearson's correlation coefficients of probe DCIC with MTG, LTG, GTG and ERTG were 0.96, 0.96, 0.87, and 0.87, respectively, which confirmed that probe DCIC can accurately locate mitochondria, lysosomes, Golgi apparatus and endoplasmic reticulum in HeLa cells.

The ability of fluorescence probe to localize mitochondria is easily affected by mitochondrial membrane potential ($\Delta\Psi_m$) [30,31]. In order to assess whether the mitochondrial localization ability of DCIC will be affected by $\Delta\Psi_m$, HeLa cells were incubated with mitochondrial depolarizing agent CCCP (carbonyl cyanide *m*-chlorophenylhydrazone), which is commonly used in cell biology [32,33], then colocalization experiment of DCIC was conducted with Mito-tracker Green. The results displayed in Fig. 5 indicated that after treatment with CCCP, the red fluorescence from DCIC was still highly overlapped with the green fluorescence of MTG. Moreover, Pearson's correlation coefficient between them is 0.86, which changed slightly compared with the control group without CCCP incubation. These results revealed that the ability of DCIC to locate mitochondria was not affected by $\Delta\Psi_m$.

In accordance with previous report [34], mitochondrial viscosity increased after CCCP treatment. A slight enhancement of fluorescence intensity of DCIC was found in CCCP-treated cells (Fig. 5). To further study the ability of DCIC to detect mitochondrial and lysosomal viscosity, DCIC-stained cells was treated with dexamethasone (DXM), an anti-inflammatory and immunosuppressive drug that could increase lysosomal and mitochondrial viscosity [34,35]. The results in Fig. 6 revealed that fluorescence intensity of DCIC in lysosome was weaker than that in mitochondria before dexamethasone treatment. However, though fluorescence intensity of DCIC in both mitochondria and lysosomes increased after dexamethasone treatment, the results of semi-quantitative analysis of intracellular fluorescence intensity showed fluorescence intensity in lysosomes increased more obviously than that in mitochondria after DXM treatment. Compared with mitochondria, lysosomes are more acidic. Therefore, before DXM treatment, on account of the protonation of nitrogen atoms in DCIC molecules, the fluorescence intensity of DCIC in lysosomes was weak, and after the increase of lysosome viscosity, fluorescence of DCIC in lysosomes obviously increased due to TICT effect. These results were also consistent with the results of spectral tests, suggesting that probe DCIC is suitable for monitoring intracellular lysosomal viscosity changes.

In summary, we have synthesized a viscosity fluorescence probe with hemicyanine structure based on molecular rotor. Probe DCIC possesses large Stokes shift, excellent selectivity, good sensitivity, near infrared emission (630 nm) and good photostability. Because the protonation of N atoms in probe DCIC, DCIC has unique pH dependence, and the fluorescence will not be quenched in alkaline environment. Cellular assessments revealed that DCIC had low cytotoxicity and could accurately locate mitochondria, lysosomes, endoplasmic reticulum and Golgi apparatus. In addition, due to the joint action of pH-dependence and TICT mechanism, DCIC can detect the change of lysosome viscosity. This probe provides a powerful tool for multi-organelle localization and lysosomal viscosity detection, and provides a promising strategy for the design of pH-dependent lysosomal viscosity fluorescence probes.

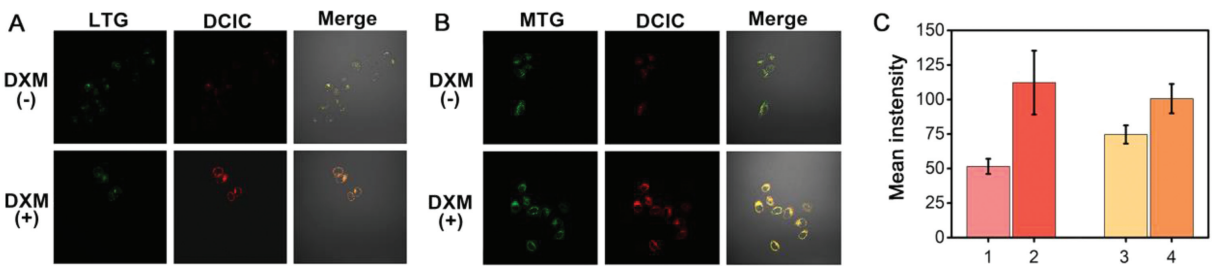

Fig. 6. Confocal microscopic images of lysosomes (A) and mitochondria (B) pretreated with DXM (20 μmol/L) and then incubated with DCIC (1 μmol/L) and Lyso-tracker Green (1 μmol/L) and Mito-tracker Green (1 μmol/L), respectively. (C) Semiquantitative analysis of fluorescence intensity: 1. HeLa cells treated with DCIC and LTG; 2. HeLa cells pretreated with DXM and then incubated with DCIC and LTG; 3. HeLa cells treated with DCIC and MTG; 4. HeLa cells pretreated with DXM and then incubated with DCIC and MTG.

Declaration of competing interest

The authors declare that they have no known competing financial interests or personal relationships that could have appeared to influence the work reported in this paper

Acknowledgments

We are grateful for the financial supports from Scientific and Technological Key Project in Henan Province (No. 22170015), National Natural Science Foundation of China (No. U1704161), Zhengzhou University (No. 32211807) and Henan Provincial Science and Technology Research Project (No. JC21253010).

Supplementary materials

Supplementary material associated with this article can be found, in the online version, at doi:10.1016/j.cclet.2022.06.049.

References

[1] R.M. Perera, R. Zoncu, Annu. Rev. Cell Dev. Biol. 32 (2016) 223–253.
[2] X. Wang, C. Yang, J. Cell Biol. 220 (2021) e202102001.
[3] M.D. Shawn, G.V.H. Matthew, Annu. Rev. Pharmacool. Toxicol. 57 (2017) 481–507.
[4] J.B. Spinelli, M.C. Haigis, Nat. Cell Biol. 20 (2018) 745–754.
[5] S. Javadov, A.V. Kozlov, A.K.S. Camara, Cells 9 (2020) 1177.
[6] X. Chen, J.R. Cubillos-Ruiz, Nat. Rev. Cancer 21 (2021) 71–88.
[7] M.J. Phillips, G.K. Voeltz, Nat. Rev. Mol. Cell Biol. 17 (2016) 69–82.
[8] N. Fatemeh, A.C. Robert, Nat. Rev. Rheumatol. 13 (2016) 25–40.
[9] T.S. Neil, G.S. Savannah, L.S. Cristina, G.P. Meares, Mol. Neurodegener. 12 (2017) 42.
[10] H. Zhu, J. Fan, J. Du, X. Peng, Acc. Chem. Res. 49 (2016) 2115–2126.
[11] J.I. Sbodio, B.D. Paul, C.E. Machamer, S.H. Snyder, Cell Rep. 4 (2013) 890–897.
[12] J. Cui, Y. Yao, C. Chen, et al., Chin. Chem. Lett. 30 (2019) 1071–1074.
[13] L. Hao, Z.W. Li, D.Y. Zhang, et al., Chem. Sci. 10 (2019) 1285–1293.
[14] P. Ning, W. Wang, M. Chen, Y. Feng, X. Meng, Chin. Chem. Lett. 28 (2017) 1943–1951.
[15] A.S. Klymchenko, Acc. Chem. Res. 50 (2017) 366–375.
[16] J. Yin, L. Huang, L. Wu, et al., Chem. Soc. Rev. 50 (2021) 12098–12150.
[17] S. Wang, B. Zhou, N. Wang, et al., Chin. Chem. Lett. 31 (2020) 2897–2902.
[18] X. Zhang, H. Yan, F. Huo, J. Chao, C. Yin, Sens. Actuators B: Chem. 344 (2021) 130244.
[19] X. Li, R. Zhao, Y. Wang, C. Huang, J. Mater. Chem. B 6 (2018) 6592–6598.
[20] L.L. Li, K. Li, M.Y. Li, et al., Anal. Chem. 90 (2018) 5873–5878.
[21] L. Wang, Y. Xiao, W. Tian, L. Deng, J. Am. Chem. Soc. 135 (2013) 2903–2906.
[22] B. Dong, X. Song, C. Wang, et al., Anal. Chem. 88 (2016) 4085–4091.
[23] P. Gautam, R. Sharma, R. Misra, et al., Chem. Sci. 8 (2017) 2017–2024.
[24] J. Li, J. Rao, K. Pu, Biomaterials 155 (2018) 217–235.
[25] F. Ding, Y. Zhan, X. Lu, Y. Sun, Chem. Sci. 9 (2018) 4370–4380.
[26] C. Yang, J. Song, Y. Ding, et al., Dyes Pigm. 191 (2021) 109377.
[27] J. Park, B. Lim, N.K. Lee, et al., Sens. Actuators B: Chem. 309 (2020) 127764.
[28] M. Grossi, M. Morgunova, S. Cheung, et al., Nat. Commun. 7 (2016) 10855.
[29] G. Niu, P. Zhang, W. Liu, et al., Anal. Chem. 89 (2017) 1922–1929.
[30] J. Li, N. Kwon, Y. Jeong, et al., ACS Appl. Mater. Interfaces 10 (2018) 12150–12154.
[31] X. Li, R. Zhang, L. Guo, et al., Anal. Chem. 91 (2019) 2672–2677.
[32] P.E.Z. Klier, J.G. Martin, E.W. Miller, J. Am. Chem. Soc. 143 (2021) 4095–4099.
[33] L. Fan, J. Ge, Q. Zan, et al., Sens. Actuators B: Chem. 327 (2021) 128929.
[34] Y.F. Wei, X.F. Weng, X.L. Sha, et al., Sens. Actuators B: Chem. 326 (2021) 128954.
[35] S. Humphries, Proc. Natl. Acad. Sci. U. S. A. 110 (2013) 14693–14698.